Friction Characteristics of Steel Pistons for Diesel Engines

Citation: Kim, Dallwoo, Akemi Ito, Yasuhiro Ishikawa, Katsuyuki Osawa, and Yoshiyuki Iwasaki. "Friction Characteristics of Steel Pistons for Diesel Engines." Journal of Materials Research and Technology 1, no. 2 (July 2012): 96–102. © 2012 Brazilian Metallurgical, Materials and Mining Association

As Published: http://dx.doi.org/10.1016/S2238-7854(12)70018-2

Publisher: Elsevier

Persistent URL: http://hdl.handle.net/1721.1/91633

Version: Final published version: final published article, as it appeared in a journal, conference proceedings, or other formally published context

Journal of Materials Research and Technology

jmr&t
Journal of Materials Research and Technology
www.jmrt.com.br

ORIGINAL ARTICLE

Friction Characteristics of Steel Pistons for Diesel Engines

Dallwoo Kim[1,*], Akemi Ito[2], Yasuhiro Ishikawa[3], Katsuyuki Osawa[4], Yoshiyuki Iwasaki[5]

[1]*Advanced Research Laboratories, Tokyo City University, Tokyo, Japan; Postdoctoral Associate, Sloan Automotive Laboratory, Department of Mechanical Engineering, Massachusetts Institute of Technology, Cambridge, United States.*
[2]*Department of Mechanical Engineering, Faculty of Engineering, Tokyo City University, Tokyo, Japan.*
[3]*Isuzu Advanced Engineering Center Limited, Japan.*
[4]*Mahle Engine Components Japan Corporation, Technical Center, Japan.*
[5]*Mahle Engine Components Japan Corporation, Product Development Department, Japan.*

Manuscript received February 8th, 2012; in revised form June 19, 2012

The use of iron pistons is increasing due to the higher power requirements of diesel truck engines. Expansion of the iron piston is a common concern. The purpose of this study is to clarify the lubrication conditions of cast iron and steel pistons. Friction of steel and cast iron pistons were measured using the floating liner method. The friction of conventional aluminum pistons was also measured for comparison in this study. The measurement of the secondary motion of each piston was carried out to analyse piston friction, and the following findings were obtained. The cast iron piston showed boundary lubrication at compression top dead center (TDC). This is presumably caused by the larger tilting angle of the piston induced by the larger piston clearance. Steel pistons showed hydrodynamic lubrication conditions at TDC and BDC through each cycle, due to a good oil supply.

KEY WORDS: Diesel engine; Friction; Lubrication; Piston secondary motion; Steel piston.

1. Introduction

Combustion engines need to improve their thermal efficiency if they are to help mitigate the green house effect. In the case of diesel engines, increasing the mean effective cylinder pressure is a practical way to improve thermal efficiency. Higher mean effective pressures cause higher thermal and mechanical loads on the engine pistons. Therefore piston materials tend to change from lightweight aluminum alloy to more durable cast iron and steel. Thus, an increase in the use of iron pistons in the future is predicted. The lubrication conditions of iron pistons have not yet been thoroughly researched[1]. This study is aimed at clarifying the lubrication conditions of iron pistons. Friction forces generated by a cast iron piston and a steel piston were measured, and compared to those of an aluminum piston, using a single cylinder DI diesel engine. The secondary motion of each of the three pistons was investigated, and compared to the measured friction force. It was found that the cast iron piston showed poorer lubrication conditions than the two other pistons but that the steel piston showed better

*Corresponding author.
E-mail address: dallwoo@mit.edu (D. Kim)

lubrication conditions than those of the aluminum piston. It seems that the piston structure and its secondary motion affected lubrication conditions.

2. Test Method

2.1 Test Engine and Test Pistons

A single cylinder heavy-duty diesel engine was used in this study. The specifications of the test engine are shown in Table 1. As shown in Fig. 1, the cylinder block was modified using a floating liner device[2] to determine piston friction forces under engine operating conditions. In addition, the test engine was equipped with a supercharger driven by an electric motor, so that any optional boost pressure (Pb) was produced regardless of engine speed. The engine operating conditions are shown in Table 2. Fig. 2 shows the test pistons. A cast iron piston (CI)[3], a steel piston (ST), and an aluminum piston (AL) were prepared. The combustion chamber of each piston had the same geometry and displacement. The difference in the piston height was adjusted by a special connecting rod so that compression ratios were regulated at 16:1. Table 2 lists the maximum skirt diameter of each piston, measured

Table 1 Test engine specifications

Engine Type	Single cylinder, 4 stroke Common Rail Diesel engine
Displacement [liter]	1.133
Bore x stroke [mm]	112 x 115
Compression ratio	16
Piston cooling	Oil jet & Cooling channel
Valve train	OHV 4 valve / cylinder
Injection nozzle	∅ 0.29 x 5 holes
Common rail pressure [MPa]	~ 150
Boost pressure [kPa]	~150
Number of injections	3 times / stroke (independently controlled)

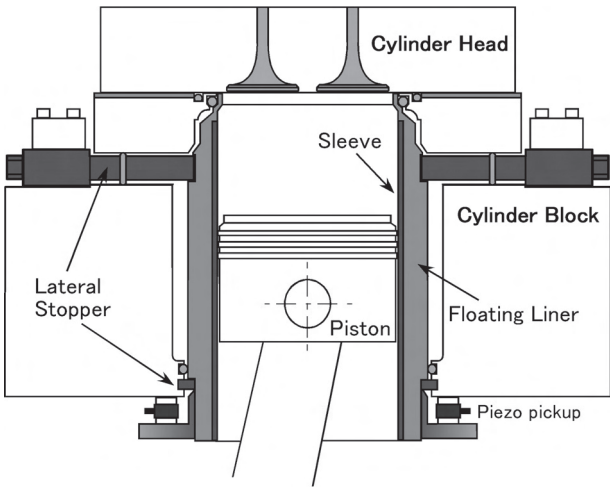

Fig. 1 Sectional view of the floating liner device.

Table 2 Skirt diameter of each test piston

Temperature	Piston		
	AL [mm]	CI [mm]	ST [mm]
At room temperature	111.90	111.94	111.97
At 50° C	111.98	111.98	112.01
At 100° C	112.12	112.01	112.04
At 150° C	112.25	112.07	112.11
At 200° C	112.37	112.17	112.18

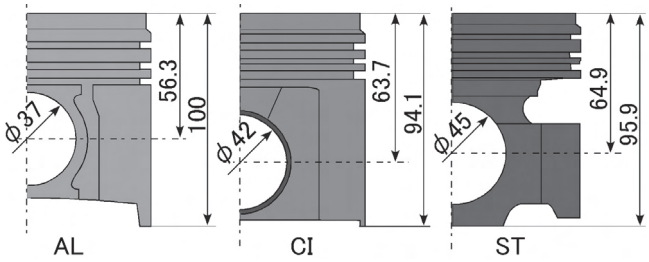

Fig. 2 Outline of test pistons.

at room temperature (50°C, 100°C, 150°C, and 200°C) using a micrometer under static conditions. For the diameter measurements, pistons were heated to a specified temperature in an electric oven, where a J type thermocouple attached to the inner face of the piston maintained the proper temperature. This static measurement of thermal expansion revealed that the CI piston and the ST piston had larger skirt clearances, by approximately 200 µm, when compared to the AL piston (at 200°C). This suggested that a thorough examination of piston friction forces and piston secondary motion was required. Table 3 lists the skirt roughness of each test piston at the thrust side (T) and at the anti-thrust side (A). As shown in Table 4, it was not possible to make the shape of the test piston rings identical for each piston, however. Total ring tension, especially oil ring tension, was regulated to almost the same level for each of the three pistons, at 47 N. Consequently, it was predicted that the effect of the piston rings on the friction forces of each piston was not substantial.

2.2 Measurement Method for Piston Secondary Motion

To determine piston secondary motion, four inductance type clearance sensors[4] per piston were attached to the thrust and anti-thrust sides (Fig. 3), and clearance between these sensors and the cylinder wall was measured. Here, the position of the clearance sensors attached to each piston was set

Table 3 Skirt roughness of each test piston after break-in

	AL		CI		ST	
	T	A	T	A	T	A
Roughness [Ra]	1.93	2.43	1.95	2.19	2.10	1.79

Table 4 Specifications of the test piston rings

AL Piston	Top ring	2nd ring	Oil ring	Total [N]
Shape	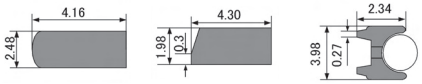			
Tension [N]	23N	19N	47N	89N
CI Piston	Top ring	2nd ring	Oil ring	Total [N]
Shape	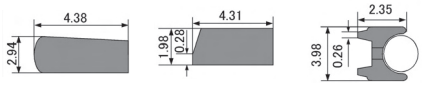			
Tension [N]	28N	19N	47N	94N
ST Piston	Top ring	2nd ring	Oil ring	Total [N]
Shape	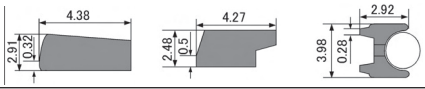			
Tension [N]	27N	18N	47N	92N

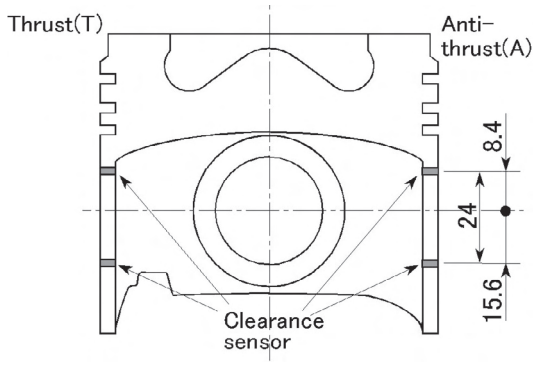

Fig. 3 Positions of clearance sensors.

identical to the center of the piston pin, where the copper wires of the clearance sensors were routed out of the engine using a linkage device (Fig. 4). Any harmful after production was not added on the piston as shown in the detail of the piston in Fig. 4.

2.3 Piston Temperature Measurement Method

Thirteen J type thermocouples per piston were installed, to investigate piston temperatures under engine operating conditions (Fig. 5). Here, the positions of the thermocouples in each piston were the same as the positions for the clearance sensors, and the thermocouples were also directed outside through the same linkage device (Fig. 4).

3. Results of Measurements

3.1 Results of Piston Friction Force Measurements

Piston friction force was measured under constant conditions where engine speed was set at 1,000 rpm, cylinder temperature was 100°C, oil temperature was 90°C, and with Pb set at both Pb = 0 kPa and Pb = 100 kPa. Fig. 6 shows the measurement values of friction forces and the

Fig. 4 Diagram of linkage device.

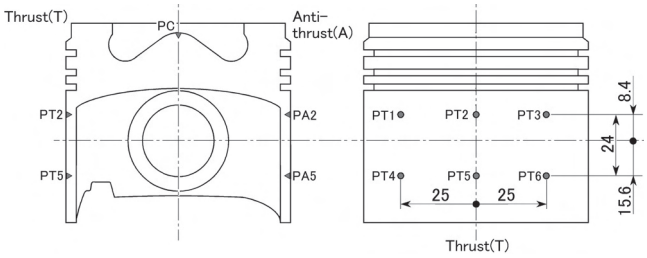

Fig. 5 Positions of thermocouple sensors.

calculated values of piston side forces of each of the AL, CI, and ST pistons without boost pressure. Fig. 7 shows those measurements with Pb.

3.1.1 Piston friction forces without boost pressure

The results of the measurement of the friction forces of the CI piston shown in the Fig. 6 suggests that its friction spike, just after the compression top dead center, was larger than that of the AL piston. This was due to a boundary lubrication condition which suggests that the lubricated condition for the piston had deteriorated by this stage of the combustion engine cycle. On the other hand, it shows that the transition

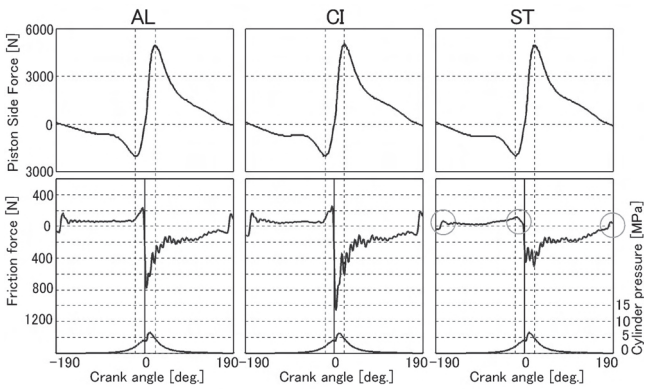

Fig. 6 The relationship between piston side forces and piston friction forces (1,000 rpm, Pb = 0 kPa).

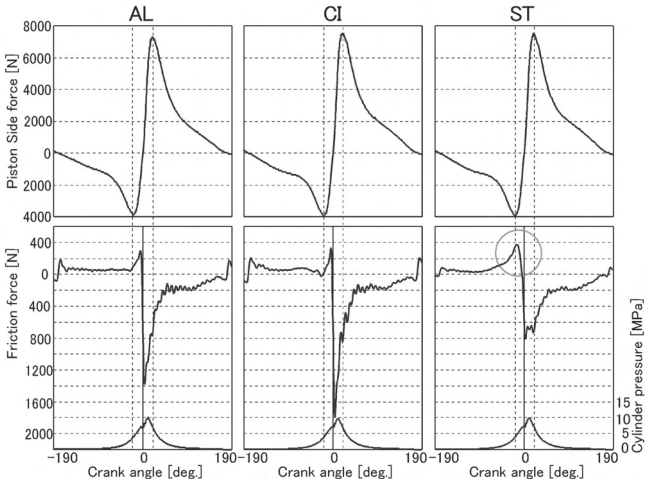

Fig. 7 The relationship between piston side forces and piston friction forces (1,000 rpm, Pb = 100 kPa).

of the friction forces in the other stages of the engine stroke was almost the same as that of the AL piston. In addition, the ST piston demonstrated a lower friction spike around compression top dead center than for the other pistons. The friction spike level differences at top and bottom dead centers, as shown by the circles in Fig. 6, are also lower, which suggests that a hydrodynamic lubrication condition was produced at top and bottom dead center stages throughout one cycle of the engine.

3.1.2 Piston friction forces with boost pressure

Fig. 7 shows the friction forces of each piston when the Pb was increased to 100 kPa. Here, the CI piston shows an even larger friction spike around compression top dead center, due to a higher Pb, which suggests a further boundary lubrication condition. In addition, the ST piston shows a lower friction spike around top dead center than any of the other pistons, as is the case without Pb. Among all of the test pistons the ST piston demonstrates the optimum capability to maintain proper lubrication. As shown in Fig. 2, the ST piston was configured such that the skirt and crown were divided to facilitate better oil supply provision to the area of the piston rings, unlike the other pistons. Also, the frictional force of Firing-TDC was smaller though h1 of the top ring is larger than AL. It seems to be a good supply of lubricant. Conversely, friction forces in the latter stage of the compression stroke increased significantly, as shown by the circle in Fig. 7. The ST piston produced different friction wave characteristics than the other pistons. The friction increase showed good agreement with increase in the piston side force. Therefore, it seemed that friction increase in the latter half of the compression stroke was due to the piston side force.

3.1.3 Comparison of friction mean effective pressure

Fig. 8 shows Friction Mean Effective Pressure (FMEP) of each piston in two conditions: with Pb (Pb = 100 kPa) and without Pb (Pb = 0 kPa). The CI piston shows the largest FMEP value, providing evidence that the boundary lubrication condition resulted in an increase in friction loss. In comparison, the ST piston shows the lowest FMEP value in the no Pb condition, which indicates that it has better friction properties than the other pistons. Nevertheless, with Pb, it shows a FMEP value similar to that of the AL piston. This is due to the increased friction forces in the half of the compression stroke. So, it was assumed that the optimization of piston skirt profile is effective on improvement of large friction force.

3.1.4 Comparison of the maximum piston side pressures

Fig. 9 shows the friction forces of each piston at crank angles where the side forces on the thrust and anti-thrust sides reach their maximum values. They were measured when Pb was present. Because the condition without Pb demonstrated

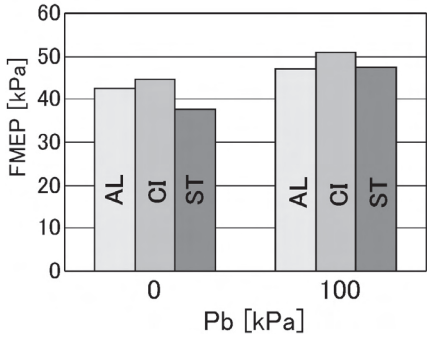

Fig. 8 Variation in FMEP of each piston.

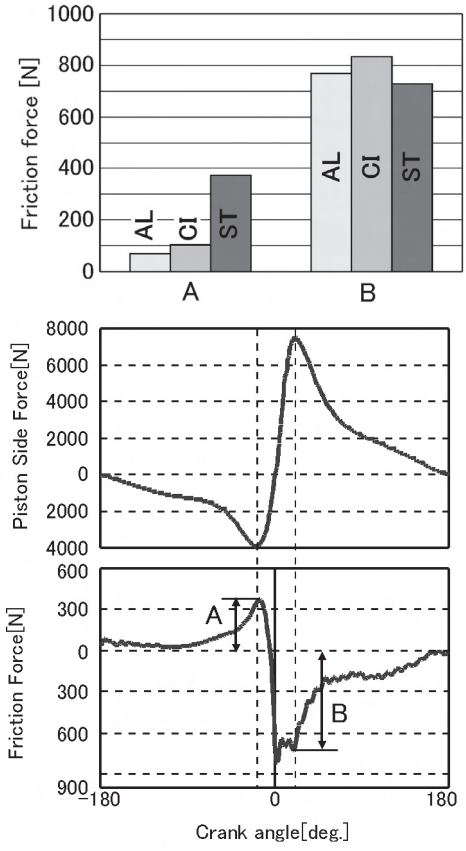

Fig. 9 Frictional force at the position of maximum side force in each piston (1,000 rpm, Pb = 100 kPa).

the same tendency, only the boost pressurized condition, in which the lubrication requirement was most critical, is shown in Fig. 9. This suggests that the friction force (A) before the compression top dead center of the ST piston is approximately three times as large as the friction force of the other pistons. Also, there is evidence that friction force (B) after compression top dead center is almost the same for all three pistons. In order to investigate the cause, the piston secondary motion of all three pistons was measured.

3.2 Results of Piston Secondary Motion Measurements

Figs. 10 and 11 show the results of piston secondary motion of the AL and CI pistons at P = 100 kPa. Fig. 12 shows enlarged diagrams for the thrust side of the AL and CI pistons near compression top dead center. The measurement of piston secondary motion revealed that the CI piston moved a longer distance when the engine was running because its clearance was larger than that of the AL piston. This behavior resulted from the difference in the coefficient of linear expansion between the two pistons. As shown in Fig. 2, the clearance of the CI piston was approximately 100 μm greater than the clearance of the AL piston when the temperature in the piston skirt was 100°C. Fig. 13 shows the presumed behavior of both pistons after compression top dead center, based on the results of piston secondary motion measurements. The outcome shown in Fig. 12 suggests that the clearance at the upper part (TU) and lower part (TL) of the skirt of the AL piston was almost the same around compression top dead center. As Fig. 13 shows, the AL piston is flush against the cylinder wall in

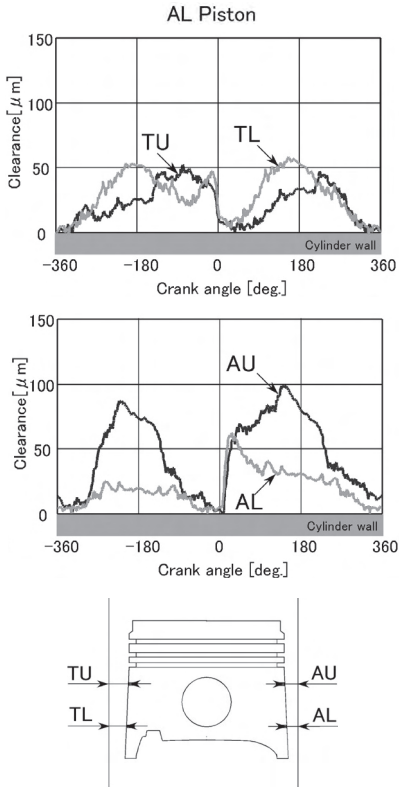

Fig. 10 AL piston secondary motion (1,000 rpm, Pb = 100 kPa).

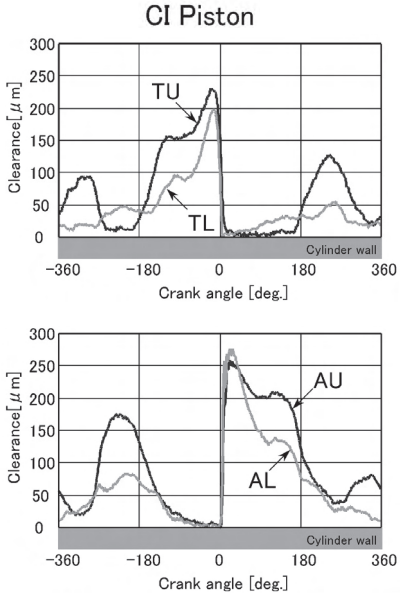

Fig. 11 CI piston secondary motion (1,000 rpm, Pb = 100 kPa).

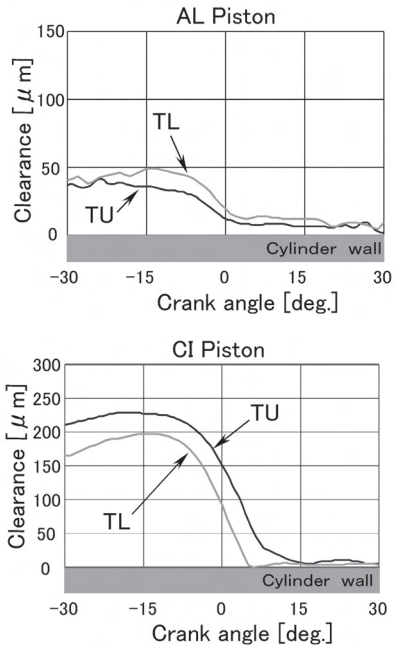

Fig. 12 Close-up of pistons secondary motion of AL and CI piston (1,000 rpm, Pb = 100 kPa).

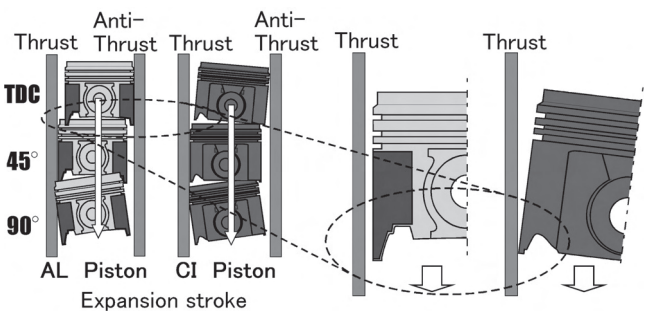

Fig. 13 Pistons behavior of AL and CI around TDC.

an almost upright position just after compression top dead center. However, unlike the AL piston, the CI piston touched the cylinder wall with its lower-skirt part first and then was in contact with the cylinder wall again just after the compression top dead center. As stated above, because the CI piston had a larger piston clearance, it moved a longer distance; we can assume it faced the cylinder wall at a higher velocity. Additionally, not only the larger clearance but also the larger top dead center compression height of the CI piston generated greater movement, to tilt the piston crown toward the anti-thrust side of the cylinder, causing the CI piston to tilt more at compression top dead center when compared to the AL piston. Hence, this suggests that the top ring was pressed toward the bottom side of the piston ring groove at compression top dead center. When the CI piston tilted significantly at compression top dead center, the top ring tilted significantly against the cylinder liner as well; we can assume that lubrication performance deteriorated under such conditions, to cause a significant increase in the friction spike when compared with the AL piston (Figs. 6 and 7). Figs. 14 and 15 show the results of the secondary motion measurements of the ST piston and its behavior around compression top dead center is estimated from the results. Fig. 16 shows diagrams comparing the behavior of the anti-thrust side of the AL piston with that of the ST piston. In the case of the ST piston, the upper part of the skirt touched the cylinder wall earlier than the lower part, at approximately 90° before compression top dead center (as indicated by "arrow B" in Fig. 14). Both upper and lower parts then touched the cylinder wall and went toward top dead center with an almost upright orientation. As shown in Fig. 16, the AL piston went upward into a position in which the lower part of the skirt contacted the liner in the latter cycle of the compression stroke, enabling the sliding surface to keep its wedge shape. In contrast, the skirt of the ST piston was kept almost parallel to the liner, which made it difficult to maintain the oil film. This is a disadvantage in terms of the oil supply; we can assume that such a condition results in an increase in the friction force, as shown by the circle in Fig. 7. Furthermore, when the ST piston traveled downward it constantly maintained a specific clearance between its skirt and the cylinder wall during its expansion stroke (as indicated by "arrow A" in Fig. 14). For the exact reason, it is not clear yet at the moment. We have to research more. But the deformation of the skirt is thought by bibliography[5]. In the case of the ST piston, the deformation seems to be the result of an area of the skirt near the side wall coming into contact with the cylinder wall because of the low stiffness of the skirt. On the other hand, when the clearance of the anti-thrust side of the ST piston on the expansion stroke is examined, the value shown is more similar to the value for the AL piston than it is to the value of the CI piston, despite a similar coefficient of linear expansion. This suggests that while the difference in clearance between the AL and CI pistons is explainable in reference to the coefficients of linear expansion because the geometry is comparatively the same, the ST piston requires further comparison with the other two pistons and an investigation which takes into account the temperature profile of the engine while running, including the heat distortion of the piston, because its configuration is significantly different from the others.

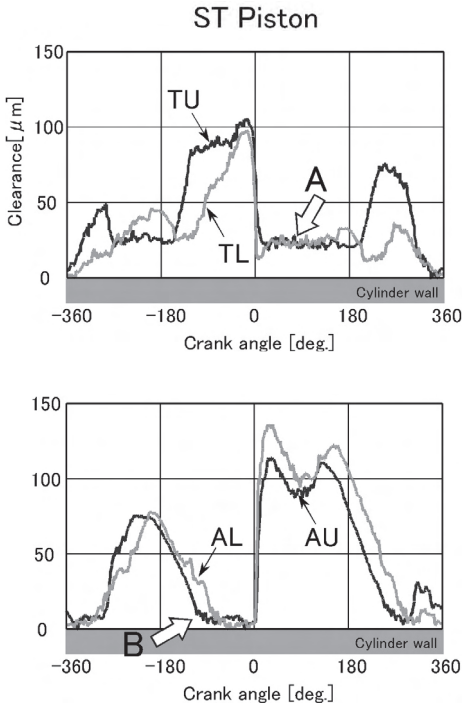

Fig. 14 ST piston secondary motion (1,000 rpm, Pb = 100 kPa).

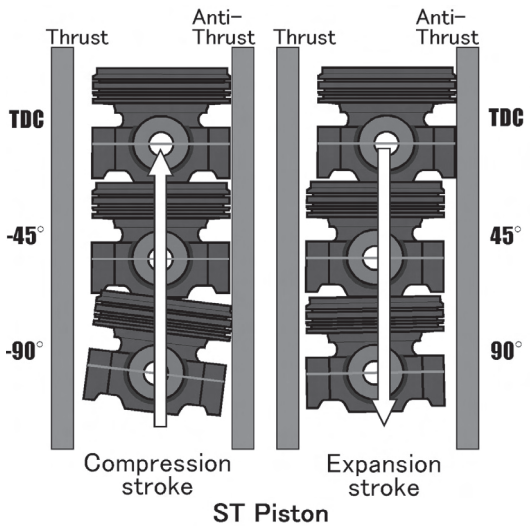

Fig. 15 Behavior of ST piston around TDC.

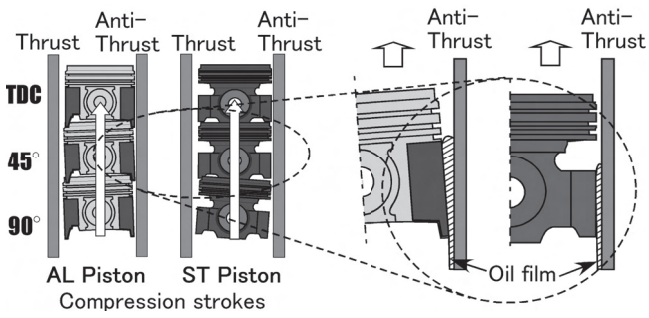

Fig. 16 AL and ST piston behavior around TDC.

3.3 Results of Piston temperature measurement

Piston temperatures were measured for the purpose of confirming that the differences in the friction forces among the pistons was due to the expansion rate of the piston skirt, in accordance to their respective temperature profiles. It was also to verify the effects of the decreased viscosity. Fig. 17 shows the results of the temperature measurements of each piston at P = 100 kPa. The fact that the temperatures of the area that forms the skirt area of the AL, CI, and ST pistons is almost the same suggests that differences in friction between each piston seem to be due to the piston skirt shape but not because of the deterioration of the oil film viscosity around the skirt area. However, the temperature in the combustion chamber of the CI and ST pistons rose significantly in comparison with the AL piston, due to differences in the thermal conductivity of the piston shapes. In addition, the reason that the friction spike of the ST piston was lower, in spite of the higher temperature in the combustion chamber (as shown in the Figs. 5 and 6) is because different piston configurations caused the oil of supply to be better or worse. However, this may result in larger oil consumption due to oil leaking into the combustion chamber via the compression ring.

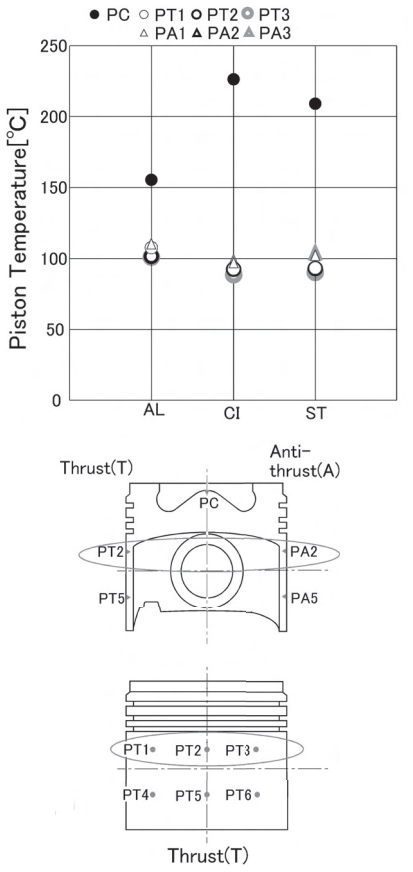

Fig. 17 Typical piston temperature of each piston (1,000 rpm, Pb = 100 kPa).

4. Conclusions

The results of the measurements and comparison of the friction forces and the secondary motion of the aluminum (AL), cast iron (CI), and steel (ST) pistons of the diesel engine produced the following conclusions:

- In a comparison with the AL piston, the CI piston demonstrated a boundary lubrication condition near compression top dead center. This may have been caused by the larger tilting angle of the piston around compression top dead center, as a consequence of a larger skirt clearance and a higher compression height, which made the top ring tilt significantly against liner, resulting in poor lubrication;
- in a comparison with other pistons, the ST piston demonstrated an optimum hydrodynamic lubrication condition at the top dead center and bottom dead center throughout one cycle of the engine. Better oil supply to the rings was provided because of the configuration of the piston;
- however, the ST piston demonstrated a notable deterioration in the lubricated condition near 20° before compression top dead center, in accordance with the rise in pressure in the cylinder when the boost pressure was raised. The reason for this is assumed to be that the oil supply to the piston skirt was interrupted because the upper part of the skirt brushed closer to the liner than the lower part did at compression top dead center;
- since the configuration of the ST piston may result in a larger consumption of oil, further investigation of the effects of piston configuration on oil consumption will be the topic of our further study.

References

1. Pan J, Nigro R, Matsuo E. 3-D Modeling of Heat Transfer in Diesel Engine Piston Cooling Galleries. SAE Technical Paper 2005-01-1644, 2005.
2. Furuhama S, Takiguchi M. Measurement of piston frictional force in actual operating diesel engine. SAE Paper nº 790855, 1979.
3. Tsujita M, Niino S, Ishizuka T, Kakinai A *et al*. Advanced Fuel Economy in Hino New P11C Turbocharged and Charge-Cooled Heavy Duty Diesel Engine. SAE Technical Paper 930272, 1993.
4. Takiguchi M, Kituchi H, Furuhama S. Influence of clearance between piston and cylinder on piston friction. SAE Paper 881621, 1988.
5. Ito A, Hitosugi H, Furuhama S. Measurement of Piston-Skirt Deformation in Engine Operation by Means of Rotating Cylinder with Gap-Sensors. SAE Technical Paper 930717, 1993.